

Tsallis Holographic Dark Energy Reconsidered

M. Dheepika*, Titus K. Mathew[†]

Department of Physics,
Cochin University of Science and Technology,
Kochi, Kerala 682022, India
*mdheepika@cusat.ac.in
†titus@cusat.ac.in

Abstract

We consider the Interacting Tsallis Holographic Dark Energy (THDE) as dynamical vacuum, with the Granda-Oliveros (GO) scale as the infrared (IR) cutoff. To probe the evolution of the spatially flat Friedmann Lemaître Robertson Walker (FLRW) universe with dark energy and matter components, we analytically solved for the Hubble parameter, and the solution traces the evolutionary path from the prior decelerated to the late accelerated epoch. We used Pantheon Supernovae type Ia and Observational Hubble Data to constrain the free parameters of the model. The estimated values of the cosmological parameters were consistent with observational results. We analysed the behaviour of the model using the statefinder and $\omega'_e - \omega_e$ plane, and the model shows a quintessence behaviour in general and approach Λ CDM in the future. We performed a dynamical analysis of the model, concluding that the prior decelerated and late accelerated phases are unstable and stable equilibria, respectively. We also investigated the thermodynamical nature of the model and found that the horizon entropy is always an increasing function of time; the generalised second law remains valid in the dynamical vacuum treatment of the model.

Keywords— Tsallis Entropy, Holographic Dark Energy, Dynamical Vacuum

1 Introduction

After the discovery of the accelerated expansion of the universe [1, 2], the desire to understand the universe spired, resulting in intensive works in recent literature. The nature and origin of the accelerated expansion of the universe is a mystery even now. Dark energy and modified theories of gravity are the two approaches that try to unwind the mystery of the universe’s accelerated expansion. One of the simplest and best dark energy models is the cosmological constant, Λ as given in the most successful model, Λ CDM. However, this model suffers mainly from two problems; one is the cosmological constant problem where there is a discrepancy in the observational and the theoretical value (10^{121} times larger) of the energy density of the cosmological constant. The other is the coincidence problem that is the unknown reason for the coincidence of matter density and the cosmological constant, despite their different evolutionary natures. Dynamical dark energy models were suggested to mitigate these problems. Some representatives of this category are quintessence [3, 4], k-essence [5], and phantom [6] models.

One of the dynamical dark energy models is the holographic dark energy (HDE) model, which pivots on the black hole thermodynamics, proposed mainly to allay the coincidence problem. The underlying idea of these models is the holographic principle [7, 8] which states that the entropy of a gravitating system is related to its surface area, not its volume. The

maximum entropy of any region of space should be less than or equal to the entropy of a black hole of similar size. The limit set by this principle implies a relation between the short distance (ultraviolet-UV) cutoff and the long distance (infrared-IR) cutoff [9]. This idea is in alliance with the quantum field theory. The initial proposal of the Holographic principle considers the entropy of the cosmological horizon as the Bekenstein-Hawking entropy and the dark energy density scales as the square of Hubble parameter. However, it could not explain the current accelerated expansion of the universe [10, 11]. HDE model with particle horizon [12, 13] as IR cutoff also could not explain the present acceleration. Taking future event horizon [13] as IR cutoff successfully explained the present accelerated expansion, but it suffered from causality problem. Since any known symmetry does not dodge the interaction between the dark sectors [14], models considering such interactions were proposed and they yield better consistency with the cosmic observations than non interacting models [15, 16, 17, 18, 19]. Granda and Oliveros proposed a new IR cutoff [11], a combined function of Hubble parameter and its time derivative, as there was a need for the new IR cutoff contrast to standard cutoffs like Hubble horizon, particle horizon and future event horizon. The resulting model successfully avoids the coincidence problem, causality problem and explains the current accelerated expansion. In order to incorporate the quantum corrections [20, 21, 22, 23, 24, 25, 26, 27, 28, 29], conventional HDE required modifications.

Tsallis and Crito [30] introduced a generalized non-additive entropy, popularly known as Tsallis entropy, to solve the thermodynamic inconsistencies in non-standard systems like black hole, and this concept is in harmony with the area law. This kind of entropy agrees well with the Friedmann equations and Padmanabhan's proposal of the emergence of space time [31]. Like in the conventional holographic dark energy model, it is possible to construct dark energy models using Tsallis entropy, and as a result, Tsallis holographic dark energy (THDE) with Hubble horizon as IR cutoff was introduced in [32]. Taking inspiration from the aforementioned study, dynamics of FRW universe having dark matter and THDE with the apparent horizon, the particle horizon, the Ricci curvature scale, or the Granda-Oliveros (GO) scale as IR cutoffs was studied considering non-interacting and interacting scenarios [33, 34, 35, 36]. It is found that the THDE model with particle horizon as IR cutoff explains the current accelerated expansion of the universe, unlike the corresponding conventional HDE model. The results from [33] show that the THDE model is not always stable for the GO scale and the Ricci scalar cutoffs in both interacting and non interacting cases. Whereas in [34] THDE model with the GO scale as IR cutoff shows stability in $(n + 1)$ dimensional FRW universe. Thermodynamical stability studies of THDE with the apparent horizon as IR cutoff in [37] shows that the model does not satisfy the stability conditions in both interacting and non interacting cases. The investigations on the evolution of the THDE with Hubble horizon as IR cutoff, by considering time varying deceleration parameter in FRW universe is discussed in [38], in Brans-Dicke cosmology is discussed in [39, 40]. Geometrical diagnosis of THDE model of the universe with the apparent horizon as IR cutoff, considering the interaction between dark sectors of the universe, was made in [41]. Cosmological model in higher dimensional Kaluza-Klien theory, having THDE with Hubble horizon as IR cutoff, and with Generalized Chaplygin Gas (GCG) as cosmic components is studied in [42]. THDE with Hubble horizon as IR cutoff in Rastall framework and on Randall-Sundrum brane has been considered in [43, 44]. Dynamical system studies on interacting and non-interacting THDE in a fractal universe with Hubble radius and apparent horizon as IR cutoff can be found in [45, 46, 47, 48]. The equivalence between Tsallis entropic dark energy and generalized HDE with cutoffs in terms of particle horizon, future horizon and its derivatives are established in [49]. Cosmological analysis of the THDE with Hubble horizon as IR cutoff

in the axially symmetric Bianchi-I universe within the framework of general relativity has been explained in [50, 51]. Sign changeable mutual interactions between dark sectors are also considered to study the effects of anisotropy in the Bianchi universe [52]. Similar analysis of THDE with Hubble horizon and GO scale as IR cutoff in Bianchi-III universe has been discussed in [53, 54]. Investigations on dynamics of THDE with Hubble horizon as IR cutoff, by assuming power law-exponential form for the scale factor have been studied in [55]. Geometrical evolutionary studies in THDE models with Hubble horizon, future event horizon, and GO scale as IR cutoffs corresponding to different interactions have been explored in [56, 57, 58, 59, 60, 61, 62, 63]. Investigations on THDE with GO scale as IR cutoff [64], presuming that this energy density is responsible for inflation, show the potentiality of the model in explaining the early universe. Comparison of THDE model with other HDE models using statefinder analysis was reviewed in [65]. The evolution of cosmological perturbations in THDE models with Hubble horizon and future event horizon as IR cutoff and Bayesian model comparison with Λ CDM as reference model has been scrutinized in [66, 67, 68]. In [69, 70, 71, 72, 73, 74, 75, 76, 77, 78, 79, 80, 81, 82, 83, 84, 85, 86], the THDE model with different IR cutoffs within various modified gravity theories and scalar field theories has also been explored. The growth rate of clustering for different IR cutoffs for the THDE model in the FRW universe can be found in [87]. Cosmological implications through non linear interactions between THDE with Hubble horizon as IR cutoff and cold dark matter in the framework of loop quantum cosmology has been discussed in [88]. Investigations on the THDE model with Hubble horizon as IR cutoff in the higher derivative theory of gravity in [89], shows that it is not compatible with late time acceleration as it could not acquire the required value of the equation of state parameter. Due to the quantified non extensivity in Tsallis entropy, studies on modification of Friedmann equation and gravity theory, including emergence proposal of gravity [90, 91, 92, 93, 94, 95] also flourish in this field. All these works were carried out considering the equation of state parameter of dark energy but as varying with the expansion of the universe.

It is to be noted that, in formulating the HDE density, one has to compare the UV cutoff, corresponding to the vacuum energy, with the IR cutoff, representing the large length scale of the universe. There is a broad consensus that the cosmological constant in the standard Λ CDM model can be the vacuum energy, having an equation of state parameter, -1 . Hence the UV cutoff involved in the HDE dark energy models may indicate that the corresponding dark energy density can better be considered a dynamical vacuum. As a result, reconsidering the THDE as a dynamical vacuum in analyzing the evolutional history of the universe is of practical significance. In the present work, we are considering the THDE as a dynamic vacuum. We study the evolution of the universe by considering the interaction, between dark matter and dark energy in conformity with the total conservation of energy, in the THDE model with the Granda-Oliveros scale as IR cutoff. Our analysis shows that the model predicts a transition to the late accelerating universe. This work also involves the geometrical and dynamical analysis and thermodynamical study of the model to check the feasibility of explaining the accelerating universe.

The structure of this paper is as follows. In the next section we present an Interacting THDE as a dynamical vacuum. We analytically solve for the Hubble parameter and investigate its evolutionary behaviour. In section 3, we constrain the parameters with observational data and discuss its cosmological implications. In section 4, we perform the dynamical analysis on the interacting THDE model using statefinder pair and $\omega'_e - \omega_e$. In section 5, we study the thermodynamical properties of the model. In the last section, we summarize the

conclusions of the work.

2 Interacting THDE Model as Dynamical Vacuum

For large scale systems, it has been shown that, the thermodynamical entropy must be modified to non-additive entropy. The investigations of quantum gravity have further supported this [26, 27]. According to Tsallis and Crito [30], the quantum correction modified the entropy-area relation as,

$$S = \gamma A^\delta, \quad (1)$$

where A is the horizon area of the black-hole, γ is a positive constant and δ is the positive non-additive parameter [30]. This will reduces to the Bekenstein entropy for $\gamma = \frac{1}{4L_p^2}$ and $\delta = 1$, with L_p^2 as the Planck length hence it is also proposed as generalizations of the Bekenstein entropy. Following the Holographic principle, Cohen et al. have found a relation between the entropy, IR cutoff (L), and the UV cutoff (Λ) as,

$$L^3 \Lambda^3 \leq S^{3/4}. \quad (2)$$

Following the Tsallis entropy in (1) and substituting for area, $A = 4\pi L^2$, leads to the relation $\Lambda^4 \leq \gamma(4\pi)^\delta L^{2\delta-4}$, and it gives a measure of the vacuum energy density. Taking consideration of the equality in this relation, a modified energy density, known as the Tsallis HDE (THDE), can be defined as,

$$\rho_{de} = CL^{2\delta-4}, \quad (3)$$

where the constant, $C = \gamma(4\pi)^\delta$ with dimension $[L^{2-2\delta}]$ (in units of $8\pi G = \hbar = c = 1$). The simplest choice for scale is $L = H^{-1}$, the Hubble horizon. In [32], authors have established that the corresponding model of the universe, with non-interacting dark sectors, can show a transition into the late time accelerated epoch. This is in contrast to conventional HDE model, which failed to predict a transition into the late accelerated epoch, if cosmic components are non-interacting.

In the present study we adopt the GO scale as IR cutoff, which was originally proposed in reference [11] to study the conventional HDE model and is given by,

$$L^{-2} = (\alpha H^2 + \beta \dot{H}), \quad (4)$$

where α and β are unknown dimensionless constants and \dot{H} , is the derivative of Hubble parameter with respect to the cosmic time. Using (4) in (3), THDE density can be written as

$$\rho_{de} = 3(\alpha' H^2 + \beta' \dot{H})^{2-\delta}, \quad (5)$$

where $\alpha' = \frac{\alpha}{3} C^{\frac{1}{2-\delta}}$ and $\beta' = \frac{\beta}{3} C^{\frac{1}{2-\delta}}$ have dimension $[L^{\frac{2-2\delta}{2-\delta}}]$.

The Friedmann equation for the flat FRW universe is given by

$$3H^2 = \rho_m + \rho_{de}. \quad (6)$$

where ρ_m and ρ_{de} is the dark matter and dark energy density respectively. The conservation equations including the interaction between THDE and dark matter are given by

$$\dot{\rho}_{de} + 3H(\rho_{de} + P_{de}) = -Q, \quad \dot{\rho}_m + 3H(\rho_m + P_m) = Q, \quad (7)$$

where $\dot{\rho}_{de}$ and $\dot{\rho}_m$ are the derivatives of dark energy and dark matter densities with respect to the cosmic time, P_{de} and P_m are the pressure of dark energy and matter respectively and Q represents the interaction, which determines the rate of exchange of energy between the dark sectors. From equation (7) it is clear that Q has to be a function of energy density and inverse of time. We are adopting a simple function, $Q = 3bH\rho_m$ where b is the coupling constant. Since the THDE is considered as a dynamical vacuum it's equation of state is $P_{de} = -\rho_{de}$ and the matter is considered as pressureless. Considering the above assumptions, the equations in (7) reduces to

$$\dot{\rho}_{de} = -3bH\rho_m, \quad \dot{\rho}_m = -3(1-b)H\rho_m. \quad (8)$$

The above equations (8) can be rewritten in terms of density parameter $\Omega = \frac{\rho}{3H_0^2}$ where H_0 denotes the present value of Hubble parameter and $x = \ln a$ as

$$\frac{d\Omega_{de}}{dx} = -3b\Omega_m, \quad (9)$$

$$\frac{d\Omega_m}{dx} = -3(1-b)\Omega_m. \quad (10)$$

The solution of equation (10) is $\Omega_m = \Omega_{m0}e^{-3(1-b)x}$ where $\Omega_{m0} = \frac{\rho_{m0}}{3H_0^2}$ is the present matter density parameter. In similar manner, $\Omega_{de0} = \frac{\rho_{de0}}{3H_0^2}$ is the present dark energy density parameter. The equation (6) can also be written as $1 = \Omega_{m0} + \Omega_{de0}$. Considering this result and using equations (10),(9) and (6), a second-order differential equation can be formulated as below

$$\frac{d^2h^2}{dx^2} + 3\frac{dh^2}{dx} + 9b\Omega_{m0}e^{-3(1-b)x} = 0. \quad (11)$$

where $h^2 = H^2/H_0^2$. The solution of the above differential equation in terms of scale factor is [96],

$$h^2 = \frac{\Omega_{m0}}{1-b}a^{-3(1-b)} + \frac{1}{3}c'a^{-3} + c'', \quad (12)$$

which tells us how the Hubble parameter evolves with respect to the scale factor of the universe. Initial conditions to evaluate the constants c' and c'' are

$$h^2|_{a=1} = 1, \quad \left. \frac{dh^2}{dx} \right|_{a=1} = \frac{2}{\beta'} \left[\left(\frac{\Omega_{de0}}{H_0^{2(1-\delta)}} \right)^{\frac{1}{2-\delta}} - \alpha' \right]. \quad (13)$$

The constants are then obtained as

$$c' = \frac{2}{\beta'} \left[\alpha' - \left(\frac{\Omega_{de0}}{H_0^{2(1-\delta)}} \right)^{\frac{1}{2-\delta}} \right] - 3\Omega_{m0}, \quad (14)$$

$$c'' = 1 - \frac{b\Omega_{m0}}{1-b} - \frac{2}{3\beta'} \left[\alpha' - \left(\frac{\Omega_{de0}}{H_0^{2(1-\delta)}} \right)^{\frac{1}{2-\delta}} \right]. \quad (15)$$

In the asymptotic limit $a \rightarrow 0$, the constant c'' can be neglected due to domination of the first two terms in the Hubble parameter equation (12) for $0 < b < 1$, consequently the resulting solution represents the decelerated expansion. In the future limit, $a \rightarrow \infty$, the

constant term in the Hubble parameter will dominate over the rest of the terms, indicating an end de-Sitter phase. Hence the model predicts a transition into a late accelerating epoch in the evolution of the universe. For $b = 0$ equation (12) will reduce to

$$h^2 = \tilde{\Omega}_{m0}a^{-3} + \tilde{\Omega}_{de0}, \quad (16)$$

where

$$\tilde{\Omega}_{m0} = \frac{2}{3\beta'} \left[\alpha' - \left(\frac{1 - \Omega_{m0}}{H_0^{2(1-\delta)}} \right)^{1/(2-\delta)} \right], \quad \tilde{\Omega}_{de0} = 1 - \tilde{\Omega}_{m0}. \quad (17)$$

This shows that, in the absence of interaction, the model is similar to that of the standard Λ CDM, but with effective mass density parameters $\tilde{\Omega}_{m0}, \tilde{\Omega}_{de0}$ [97]. Even though the dark energy density in equation (5) is varying with H , the behaviour of it as effective vacuum energy with equation of state, $\omega_{de} = -1$ is the primary reason for this Λ CDM like behaviour, in the absence of the interaction. Further, the coupled conservations equations in (7) become independent conservations, in which matter and dark energy are separately conserved. Under such a condition, the dark energy density, equivalent to the vacuum energy density, will effectively become a constant.

3 Observational Constraints and its Cosmological Implications

In this section, we estimate the constant model parameters, $\delta, \alpha', \beta', b, H_0$ and Ω_{m0} using statistical χ^2 minimisation technique by contrasting the model with cosmological observational data. The data set consists of the Type Ia supernovae data [98], and the observational Hubble data (OHD) [99, 100].

We use the latest supernovae data, the Pantheon Sample, which comprises 1048 SNe Ia data points in the redshift range of $0.01 < z < 2.3$. The luminosity distance of SN Ia can be obtained using the relation,

$$d_L(\delta, \alpha', \beta', b, H_0, \Omega_{m0}, z_i) = c(1 + z_i) \int_0^{z_i} \frac{dz'}{H(\delta, \alpha', \beta', b, H_0, \Omega_{m0}, z')}, \quad (18)$$

where z_i is the redshift of the SN Ia, c is the speed of light and $H(\delta, \alpha', \beta', b, H_0, \Omega_{m0}, z')$ is the Hubble parameter in terms of model parameters and redshift. The theoretical distance modulus of SN Ia is given by

$$\mu_{th}(\delta, \alpha', \beta', b, H_0, \Omega_{m0}, z_i) = 5 \log_{10} \left[\frac{d_L(\delta, \alpha', \beta', b, H_0, \Omega_{m0}, z_i)}{Mpc} \right] + 25. \quad (19)$$

The χ^2 function of SN Ia data can be expressed as

$$\chi^2(\delta, \alpha', \beta', b, H_0, \Omega_{m0}, M)_{SN Ia} = \sum_{i=1}^n \frac{[\mu_{th}(\delta, \alpha', \beta', b, H_0, \Omega_{m0}, z_i) - \mu_i]^2}{\sigma_i^2}, \quad (20)$$

where $\mu_i = m - M$ is the observational distance modulus of SN Ia, m and M are the apparent and the absolute magnitude of the SN Ia, $n = 1048$, the total number of data points and σ_i^2 is the variance of i^{th} measurement.

Another independent observable we use is the Hubble dataset consisting of 36 $H(z)$ data-points in the redshift range of $0.07 \leq z \leq 2.36$, out of which 31 data are determined using

the cosmic chronometric technique, 3 data from the radial BAO signal in the galaxy distribution and 2 data from the BAO signal in the Lyman forest distribution alone or cross correlated with QSOs [99]. The following χ^2 function is minimised for this Hubble parameter measurement

$$\chi^2(\delta, \alpha', \beta', b, H_0, \Omega_{m0})_{OHD} = \sum_{i=1}^n \frac{[H(\delta, \alpha', \beta', b, H_0, \Omega_{m0}, z) - H_i]^2}{\sigma_i^2}, \quad (21)$$

where H_i is the observational Hubble parameter measurement and σ_i^2 is the variance of i^{th} measurement. Combining the type 1a supernovae data and the OHD, the total χ^2 function takes the form

$$\chi_c^2 = \chi^2(\delta, \alpha', \beta', b, H_0, \Omega_{m0}, M)_{SN1a} + \chi^2(\delta, \alpha', \beta', b, H_0, \Omega_{m0})_{OHD}. \quad (22)$$

Data	Estimated values of parameters						
	δ	b	α'	β'	Ω_{m0}	H_0	M
Pantheon+OHD	1.026	$0.026^{+0.022}_{-0.021}$	$0.996^{+0.004}_{-0.004}$	$0.297^{+0.010}_{-0.009}$	$0.300^{+0.005}_{-0.004}$	$69.246^{+0.204}_{-0.206}$	-19.380

Table 1: The best estimated values and 68.3% confidence limit for Interacting THDE model parameters.

The estimated values of the model parameters using the Pantheon sample and OHD are given in Table 1. The minimum χ_c^2 is obtained as 1053.68. The $\chi_{dof}^2 = \frac{\chi_{min}^2}{n-n_p}$ is the minimum χ^2 function per degrees of freedom where n is the number of data points and n_p is the number of model parameters. The χ^2 goodness of fit, $\chi_{d.o.f.}^2 = 0.978$ i.e., around unity. The estimated value of coupling constant is obtained to be positive that in turns contribute a positive interaction term. Hence the energy transfer is from THDE to dark matter and thereby satisfying the Le Chatelier-Braun principle [101, 47].

3.1 Cosmological Parameters and statefinder diagnostic

3.1.1 Evolution of Cosmological Parameters

Estimation of luminosity and redshift from the cosmological observables contributes to the determination of present Hubble parameter of the universe. Here, we studied the background evolution of the Hubble parameter making use of the Interacting THDE solution. The evolution of the Hubble Parameter with respect to the red shift along with the 36 $H(z)$ data points is obtained as shown in Figure 2. The Hubble parameter decreases as the cosmic time evolves and the present value of the Hubble parameter is obtained as $69.246 \text{ kms}^{-1}\text{Mpc}^{-1}$ which is slightly lower than the observational value $H_0 = 70.5 \pm 1.3 \text{ kms}^{-1}\text{Mpc}^{-1}$ from WMAP + BAO + SN data [102] and slightly higher than observational value $H_0 = 67.37 \pm 0.54 \text{ kms}^{-1}\text{Mpc}^{-1}$ from Planck data [103] assuming ΛCDM model. The evolution of apparent magnitude with respect to the red shift along with the 1048 SNe Ia data points is shown in

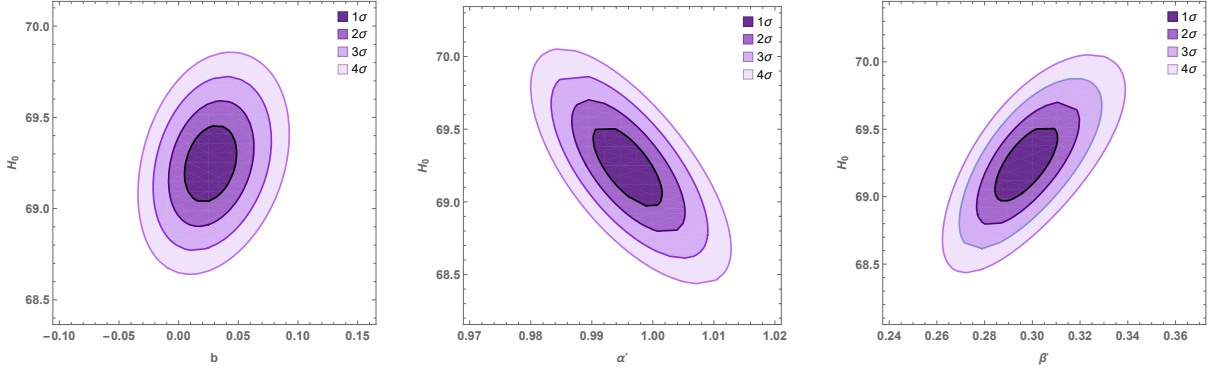


Figure 1: The confidence intervals of Interacting THDE model parameters b, α', β' using the Pantheon sample and OHD. These intervals corresponds to the 68.3%, 95.4%, 99.73% and 99.99% probabilities. The best fitted values of the model parameters with 1σ corrections are specified in Table 1

Figure 3. Both the error bar plots shows proximity between theoretical and observational results.

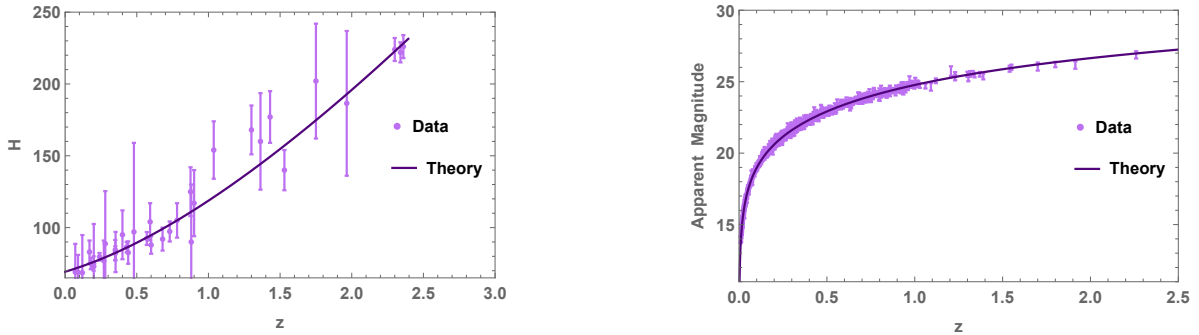


Figure 2: The evolution of Hubble parameter parameter with redshift for the best estimated values of the model parameters along with $H(z)$ data points.

Figure 3: The evolution of apparent magnitude with redshift for the best estimated values of the model parameters along with type Ia SNe data points.

The deceleration parameter which measures the rate of cosmic expansion is obtained in the following form

$$q = -1 - \frac{\dot{H}}{H^2} = -1 + \frac{3\Omega_{m0}(1+z)^{3(1-b)} + c'(1+z)^3}{2\Omega_{m0}(1+z)^{3(1-b)} + \frac{2}{3}c'(1+z)^3 + 2c''}. \quad (23)$$

In the limit $z \rightarrow -1$, the deceleration parameter $q \rightarrow -1$ and in the limit $z \rightarrow \infty$, the deceleration parameter will tend to a positive value since second term in equation (23) dominates in that case. The evolution of the deceleration parameter $q(z)$, as a function of z , for the best estimated model parameters from the combined dataset Pantheon + OHD is plotted in Figure 4. It's lucid from the figure that the model explains the current accelerated universe and also the transition from the prior decelerated phase to the present accelerated phase. The transition redshift z_t (*i.e.*, $q(z_t) = 0$) is found to be 0.75, which is slightly greater than

the transition redshift obtained for Interacting THDE model with Hubble horizon and future event horizon as IR cutoff ($z_t = 0.634_{-0.045}^{+0.051}$ and $z_t = 0.649_{-0.025}^{+0.010}$ respectively) [104]. The current value of deceleration parameter ($q_0 = q(z)|_{z=0}$) obtained for the estimated values of the model parameters is $q_0 = -0.568$, is closer to the observational value $q_0 = -0.63 \pm 0.12$ from Λ CDM based CMB priors [105]. Our estimated cosmological parameter values are in good concordance with previous results from model independent methods, parametric reconstruction techniques as well as other dark energy models mentioned in [106, 107, 108, 109].

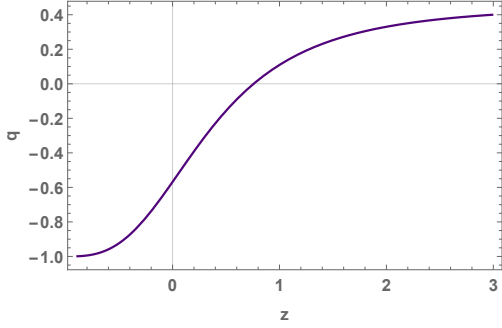


Figure 4: The evolution of deceleration parameter with redshift for the best estimated values of the model parameters.

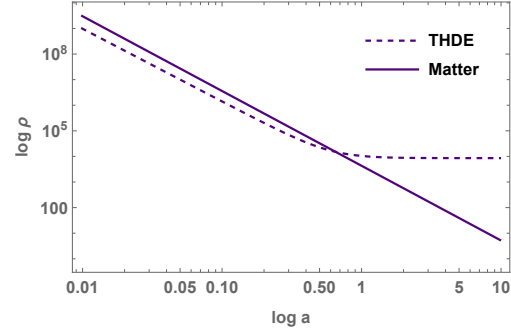


Figure 5: Evolution of matter density and THDE density with scale factor of the universe in logarithmic scale

A juxtaposition of the evolution of matter density parameter and THDE density parameter in logarithmic scale is shown in Figure 5. This very well implies that the universe will be dominated by THDE in the future. The evolution of the densities of matter and dark energy are comparable with each other for the high redshift values even though the matter density is dominating in early universe and is diminishing in late phase of the universe, that solves the coincidence problem as the acceleration began at low redshifts and this is well demonstrated in the Figure 5. The current value of the matter density parameter is obtained as $\Omega_{mo} = 0.300$ from the best fit values of parameters, is slightly lower than the observational value $\Omega_{mo} = 0.3147 \pm 0.0074$ from Planck data [103].

3.1.2 The Age of the Universe

The age of the universe can be estimated to a certain level of accuracy using the present cosmological observational data even though systematic and statistical uncertainties will arise during the course of observation and estimation. Theoretically, considering the interacting THDE model the age of the universe can be calculated by slightly rearranging the equation (12) and the resultant equation takes the form

$$H = \frac{\dot{a}}{a} = H_0 \left(\frac{\Omega_{m0}}{1-b} a^{-3(1-b)} + \frac{1}{3} c' a^{-3} + c'' \right)^{\frac{1}{2}}. \quad (24)$$

Above equation can be solved by considering the value of scale factor $a = 0$ for the big bang time t_b and $a = 1$ for the present time t_0 . The age of the universe is estimated as

$$t_0 - t_b = 0.9945 H_0^{-1}. \quad (25)$$

Using the best estimated values of the parameters from the combined data the age of the universe is evaluated as 14.05 Gyrs which is slightly lower than the age calculated for Interacting THDE model with future event horizon as IR cutoff ($14.20_{-0.32}^{+0.18}$ Gyrs) and slightly

greater than the age calculated for Interacting THDE model with Hubble horizon as IR cutoff ($13.71^{+0.24}_{-0.41}$ Gyrs, upper bond of 13.43 and lower bond of 13.04 Gyrs) [104, 110]. Our results is closer to the standard value of age 13.8 ± 0.02 Gyrs obtained from Planck mission and 13.72 ± 0.12 Gyrs from WMAP + bao + SN data assuming Λ CDM model [103, 102] and $13.5^{+0.16}_{-0.14}(\text{stat.}) \pm 0.23(0.33)(\text{sys.})$ Gyrs from the oldest globular cluster [111].

3.1.3 Evolution in $r - s$ Plane and $\omega'_e - \omega_e$ Plane

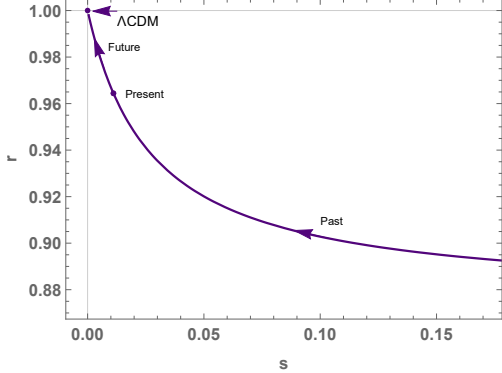


Figure 6: The statefinder evolutionary trajectory for interacting THDE in the $r - s$ plane for the best estimated values of the model parameters.

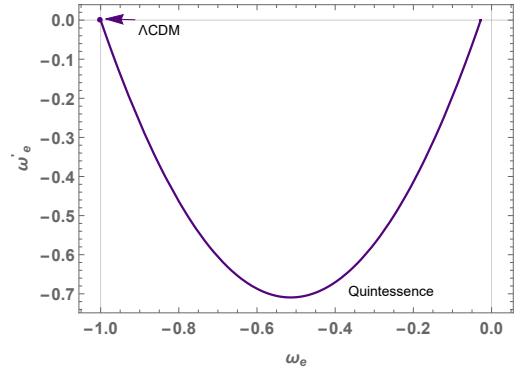


Figure 7: The evolutionary trajectory for interacting THDE in the $\omega'_e - \omega_e$ plane for the best estimated values of the model parameters.

To check further, the reliability of THDE model being a generalized model of dark energy in contrast to the present observational data we studied the evolution using the geometrical pair called the statefinder pair $\{r, s\}$ constructed from the scale factor and its derivatives, first defined by Sahni et al. [112, 113]. The relationship connecting the statefinder pairs and the scale factor of the universe are given by

$$r = \frac{\ddot{a}}{aH^3}, \quad s = \frac{r - 1}{3(q - \frac{1}{2})}. \quad (26)$$

It is lucid from (26), r is third order derivative of ' a ' and s is related to ' r ' and ' q ' linearly. The statefinder pair $\{r, s\}$ can also be expressed in terms Hubble parameter and it's derivatives as

$$\begin{aligned} r &= \frac{1}{2h^2} \frac{d^2h^2}{dx^2} + \frac{3}{2h^2} \frac{dh^2}{dx} + 1, \\ s &= -\frac{\frac{1}{2} \frac{d^2h^2}{dx^2} + \frac{3}{2h^2} \frac{dh^2}{dx}}{\frac{3}{2h^2} \frac{dh^2}{dx} + \frac{9}{2}}. \end{aligned} \quad (27)$$

Using equation (12) in the above equations will results in the following two expressions in terms of model parameters

$$\begin{aligned} r &= 1 - \frac{9b\Omega_{m0}a^{-3(1-b)}}{2(\frac{\Omega_{m0}}{1-b}a^{-3(1-b)} + \frac{1}{3}c'a^{-3} + c'')}, \\ s &= \frac{b\Omega_{m0}a^{-3(1-b)}}{c'' + \frac{b}{1-b}\Omega_{m0}a^{-3(1-b)}}. \end{aligned} \quad (28)$$

The parametric plot of $\{r, s\}$ is obtained as shown in figure 6. Using this diagnostics THDE model can be differentiated from the Λ CDM model. The statefinder pair $\{r, s\}$ for Λ CDM

is $\{1, 0\}$. Applying the limit $a \rightarrow \infty$, shows that the $\{r, s\}$ pair for the model approaches $\{1, 0\}$. Thus this model approaches Λ CDM asymptotically at late times. The present value of $\{r, s\}$ pair from the evolution trajectory of the model is obtained as $\{0.964, 0.011\}$. For the quintessence models the $\{r, s\}$ pair lies in $r < 1$ and $s > 0$. The trajectory in it's early phase shows aforesaid behavior.

In addition, we have obtained the effective equation of state parameter using the relation,

$$\omega_e = \frac{P}{\rho} = -1 - \frac{2\dot{H}}{3H^2}, \quad (29)$$

where P and ρ are the effective pressure and energy density respectively. Using the equation (12) in (29) the effective equation of state parameter for this model takes the following form

$$\omega_e = -1 + \frac{3\Omega_{m0}e^{-3(1-b)x} + c'e^{-3x}}{\frac{3\Omega_{m0}}{1-b}e^{-3(1-b)x} + c'e^{-3x} + 3c''}. \quad (30)$$

The asymptotic limit of this is as follows. As $x \rightarrow -\infty$, the effective equation of state becomes, $\omega_e \rightarrow 0$ and as $x \rightarrow +\infty$ the $\omega_e \rightarrow -1$. In the prior case the matter component could be the dominant component while in the later accelerated epoch, the dominant component is the dark energy. The derivative of ω_e with respect to x is obtained to be

$$\omega'_e = \frac{3(3\Omega_{m0}e^{-3(1-b)x} + c'e^{-3x})^2}{(\frac{3\Omega_{m0}}{1-b}e^{-3(1-b)x} + c'e^{-3x} + 3c'')^2} - \frac{3(\frac{3\Omega_{m0}}{1-b}e^{-3(1-b)x} + c'e^{-3x} + 3c'')(3(1-b)\Omega_{m0}e^{-3(1-b)x} + c'e^{-3x})}{(\frac{3\Omega_{m0}}{1-b}e^{-3(1-b)x} + c'e^{-3x} + 3c'')^2}. \quad (31)$$

The evolutionary trajectory of the model in the phase plane of $\omega'_e - \omega_e$, the effective equation of state parameter and it's derivative, is depicted in Figure 7. The Λ CDM model in $\{\omega'_e - \omega_e\}$ plane is $\{-1, 0\}$. It complements the results from statefinder analysis by showing that the trajectory is initially confined in the quintessence region $\omega_e > -1$, $\omega'_e < 0$ and approaches Λ CDM in the late time as $\omega_e \rightarrow -1$, $\omega'_e \rightarrow 0$.

The statefinder analysis of an Interacting THDE with Hubble horizon as IR cutoff for $1 < \delta < 2$ and $\delta > 2$ in [57] shows that in the same interval of δ model behaves differently while considering different interactions between dark sectors using SNe + BAO + OHD + CMB. It shows that the evolutionary trajectories lies in both quintessence and phantom region and it is complimented by the results from $\omega'_T - \omega_T$ plane. Similar results are found in [61] for interacting THDE with apparent horizon as IR cutoff. There, in the absence of interaction their model approaches Λ CDM and as the interaction increases the distance of approach to the Λ CDM increases. But in the absence of interaction our model mimics Λ CDM and in the presence of interaction our model approaches Λ CDM in far future. Our results are matching with the results from statefinder parameter planes and $\omega' - \omega$ of THDE model with Hubble horizon as IR cutoff [58].

4 Dynamical Analysis of Interacting THDE Model

The dynamical system analysis enables us to see whether the model shows the stable evolution consistent with the observations. For the phase space analysis of the model, a set of

dimensionless variables is introduced as follows:

$$u = \frac{\rho_m}{3H^2}, \quad v = \frac{\rho_D}{3H^2}. \quad (32)$$

The autonomous equations in terms of phase space variables can be obtained using the Friedmann equations as,

$$u' = u^2 - 6uv + (3b - 1)u, \quad (33)$$

$$v' = \frac{(2 - \delta)[2(\alpha' - \beta')(v^2 - v) - uv((\alpha' - \beta') + \frac{3\beta'}{2}(3b - 1))]}{\alpha' + \beta'(v - \frac{u}{2} - 1)} - 2v^2 + uv + 2v, \quad (34)$$

where prime ('') denotes differentiation with respect to $x = \ln a$. Both the equations are functions of u and v . By equating $u' = 0$ and $v' = 0$, the real and physically meaningful critical points obtained are $(\tilde{u}, \tilde{v}) = (0, 1), (1 - 3b, 0)$ and they corresponds to the de Sitter phase and the matter dominated phase respectively.

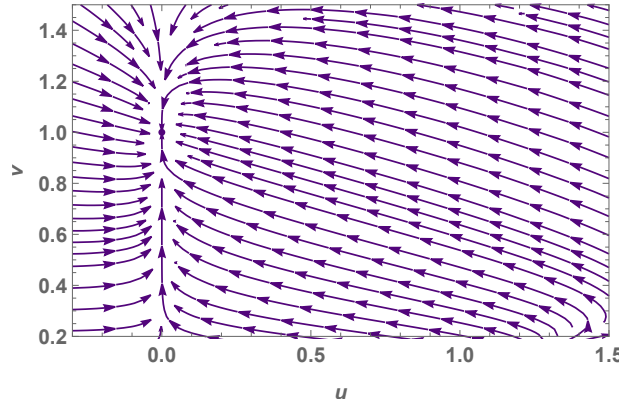


Figure 8: The evolution of the phase space trajectories in the $u - v$ plane for the best estimated model parameters

The behavior of the trajectory near the critical points can be analysed by considering the small neighbourhood of critical points as

$$u = \tilde{u} + \xi, \quad v = \tilde{v} + \eta. \quad (35)$$

in which ξ and η are small compared to \tilde{u} and \tilde{v} . Linearizing the set of equations 32 and 33 with respect to ξ and η , will result in a matric equation

$$\begin{bmatrix} \xi' \\ \eta' \end{bmatrix} = \begin{bmatrix} \left(\frac{\partial u'}{\partial u}\right)_{(\tilde{u}, \tilde{v})} & \left(\frac{\partial u'}{\partial v}\right)_{(\tilde{u}, \tilde{v})} \\ \left(\frac{\partial v'}{\partial u}\right)_{(\tilde{u}, \tilde{v})} & \left(\frac{\partial v'}{\partial v}\right)_{(\tilde{u}, \tilde{v})} \end{bmatrix} \begin{bmatrix} \xi \\ \eta \end{bmatrix}, \quad (36)$$

where 2×2 matrix on the right hand side of the above equation is the Jacobian at the critical points corresponding to the autonomous system and the partial derivatives are calculated about the critical points (\tilde{u}, \tilde{v}) .

Critical points	Eigen values	Nature
(0,1)	(-2.921, -0.633)	Stable
(0.921, 0)	(0.921, 0.038)	Unstable

Table 2: Critical points and stability of the corresponding eigen values calculated using the best estimated model parameter values.

The eigen values of the 2×2 Jacobian matrix can be obtained by diagonalizing the matrix and it's nature decides the asymptotic stability nature of critical points. The critical points (equilibrium points) can be source point or past attractor if the eigenvalues were positive quantities, or a saddle point if at least one of the eigenvalues were of a different sign, and future attractor if all the eigenvalues were negative quantities [114]. The eigen values corresponding to the Jacobian matrix are evaluated and are given in Table 2.

The critical point $(0, 1)$, for which dark energy is the dominant component, is stable since both it's eigen values are negative. This represents a future stable point. The convergence of all trajectories to the future attractor at $(0, 1)$ is well depicted in the Phase space diagram shown as Figure 8. Universe undergoes a de Sitter expansion at this point. Similar results are found for a linearly interacting THDE with Hubble horizon as IR cutoff [110]. The critical point $(0.921, 0)$, for which matter is the dominant component, is unstable since both it's eigen values are positive. All trajectories diverges from $(0.921, 0)$ and that is clear from Figure 8. This shows that the system emerges from a decelerated expansion and ends up in on a de Sitter epoch.

5 Thermodynamics of Interacting THDE Model

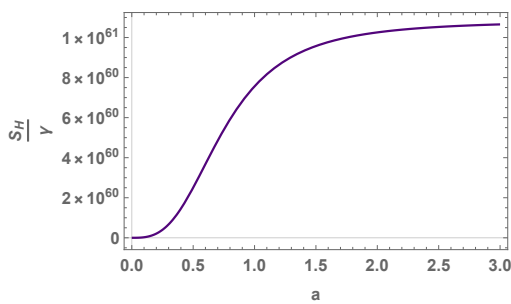


Figure 9: The evolution of $\frac{S_H}{\gamma}$ with scale factor.

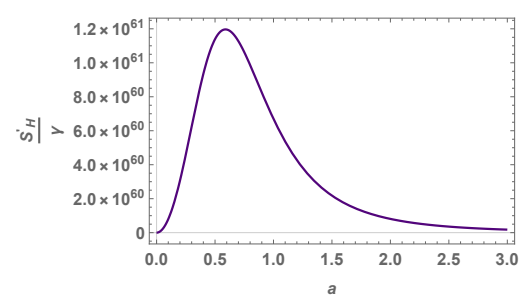


Figure 10: The evolution of $\frac{S'_H}{\gamma}$ with scale factor.

Any isolated macroscopic systems advances to the maximum entropy state in compliance with the constraints as per the generalized second law (GSL) of thermodynamics [115]. From the aforesaid statement it can be deduced that the entropy S , of isolated systems cannot decrease, i.e., $S' \geq 0$, where the prime means derivative with respect to the scale factor a and it must be a convex function of the scale factor, $S'' < 0$, atleast at the last juncture of the evolution so that the system attains a stable equilibrium state.

In the present work, we consider Tsallis entropy as the horizon entropy in place of the standard Bekenstein-Hawking entropy. Thus the horizon entropy takes the form

$$S_H = \gamma A^\delta, \quad (37)$$

where $A = 4\pi r_H^2$ is the horizon area with apparent horizon radius $r_H = \frac{c}{H}$. Then the equation (37) becomes

$$S_H = \gamma \left(\frac{4\pi c^2}{H^2} \right)^\delta k_B, \quad (38)$$

where c is the velocity of light and k_B is the Boltzmann constant. The evolution of $\frac{S_H}{\gamma}$ with respect to the scale factor is shown in Figure 9. The rate of change of horizon entropy with respect to scale factor is given by

$$S'_H = \gamma (4\pi c^2)^\delta \left(\frac{-2\delta H'}{H^{2\delta+1}} \right). \quad (39)$$

Since the Hubble parameter is a steep decreasing function with scale factor, it's variation, $H' < 0$, always. As a result the first derivative of the entropy, S'_H will always greater than zero, and hence the entropy will always increase. The second derivative of horizon entropy with respect to the scale factor is given by

$$S''_H = 2\gamma\delta (4\pi c^2)^\delta \left[(2\delta + 1) \left(\frac{H'}{H^{\delta+1}} \right)^2 - \frac{H''}{H^{2\delta+1}} \right]. \quad (40)$$

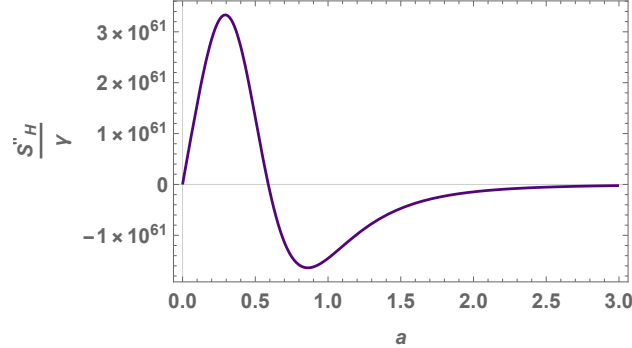


Figure 11: The evolution of $\frac{S''_H}{\gamma}$ with scale factor.

The numerical simulations [116, 117] on the observational data [118, 119] on Hubble parameter shows that $H' < 0$ and $H'' > 0$. The variation of $\frac{S'_H}{\gamma}$ with scale factor with a initial rise representing the monotonic increase in the horizon entropy during the prior decelerated stage and a fall corresponding to the decrease in entropy during the accelerated phase is well protayed in Figure 10. Finally in the asymptotic limit $a \rightarrow \infty$ it approaches zero corresponding to the attainment of equilibrium state by the universe. Nevertheless this always indicate that the entropy always increases. The behavior of $\frac{S''_H}{\gamma}$ with scale factor in Figure 11 guarantees the convexity thereby ensuring that entropy doesn't grow unboundedly. The generalized second law of thermodynamics stipulates that the entropy of the horizon together with the entropy of the matter inside the horizon must always increase with time [120]. Since it is clear the matter entropy is much less than the horizon entropy (smaller in the order of 35) [121, 122], the total entropy can approximately be taken as the horizon

entropy. Since the horizon entropy is an increasing function as shown in Figure 9, the generalized second law of thermodynamics is satisfied. Though few studies considering DE with varying equation of state in the literature shows the plausibility of violation of GSL depending on the evolution of the universe [47], tracing back the DE to a dynamical vacuum model would spare us from violating the generalised second law of thermodynamics.

6 Conclusion

In the present work, we have analysed Interacting Tsallis Holographic Dark Energy (THDE) as Dynamical vacuum to explain the recent accelerated cosmic expansion. We have considered Granda Oliveros (GO) scale, a function of Hubble parameter and it's time derivative, as IR cutoff. The interaction between the dark sectors have been accounted through a simple form of interaction term $Q = 3bH\rho_m$.

An exact solution for the Hubble parameter in terms of scale factor was obtained by analytically solving the Friedmann equation with the energy conservation equation. The solution successfully explains the prior decelerated expansion and the late time accelerated expansion under the asymptotic limits, hence effectively elucidating the transition. We have imposed the observational constraints on the cosmological parameters of Interacting THDE model using the Pantheon sample and the OHD. The estimated current value of the Hubble parameter and the matter density parameter are consistent with the observational results. The value of the coupling constant is positive and hence it obeys the Le Chatelier-Braun principle.

The cosmological evolution of the deceleration parameter shows that the end phase will be a de Sitter one, $q \rightarrow -1$ as $z \rightarrow -1$ and the transition from prior matter dominated epoch to the late THDE dominated epoch is found to occur at a redshift around $z_t \sim 0.75$. The studies on expansion profile of the THDE density and the matter density explains the dominating and diminishing nature of the matter density in the early phase and late phase respectively and along with that a comparable nature of evolution of THDE in the early phase removes the coincidence problem. The universe's age that can be intuited from the Interacting THDE model is around 14.05 Gyrs from the best estimated values of model parameters. Recent observations do subsistence the results.

The diagnosis of the Interacting THDE model is carried out using the statefinder analysis and the $\omega'_e - \omega_e$ pair. The evolutionary trajectory of the Interacting THDE model shows a quintessence behavior in the early phase and approaches Λ CDM in the far future. The trajectories of the $\omega'_e - \omega_e$ affirms the results from the statefinder diagnostics. The critical points obtained from the phase space analysis of the model shows that the de sitter phase is a stable equilibrium and matter dominated phase is an unstable equilibrium. Thus the dynamical system analysis of the Interacting THDE model portrays a consistent background evolution of the universe from the prior decelerated phase to the late accelerated phase. The thermodynamical analysis of THDE model shows that the horizon entropy increases with cosmic time and the generalised second law of thermodynamics remains valid in the dynamical vacuum treatment of the model.

References

- [1] A. G. Riess *et al.*, “Observational evidence from supernovae for an accelerating universe and a cosmological constant,” *Astron. J.*, vol. 116, pp. 1009–1038, 1998.
- [2] S. Perlmutter *et al.*, “Measurements of Ω and Λ from 42 high redshift supernovae,” *Astrophys. J.*, vol. 517, pp. 565–586, 1999.
- [3] R. R. Caldwell, R. Dave, and P. J. Steinhardt, “Cosmological imprint of an energy component with general equation of state,” *Phys. Rev. Lett.*, vol. 80, pp. 1582–1585, 1998.
- [4] I. Zlatev, L. Wang, and P. J. Steinhardt, “Quintessence, cosmic coincidence, and the cosmological constant,” *Physical Review Letters*, vol. 82, no. 5, p. 896, 1999.
- [5] C. Armendariz-Picon, V. F. Mukhanov, and P. J. Steinhardt, “A Dynamical solution to the problem of a small cosmological constant and late time cosmic acceleration,” *Phys. Rev. Lett.*, vol. 85, pp. 4438–4441, 2000.
- [6] R. R. Caldwell, “A Phantom menace?,” *Phys. Lett. B*, vol. 545, pp. 23–29, 2002.
- [7] G. ’t Hooft, “Dimensional reduction in quantum gravity,” *Conf. Proc. C*, vol. 930308, pp. 284–296, 1993.
- [8] L. Susskind, “The World as a hologram,” *J. Math. Phys.*, vol. 36, pp. 6377–6396, 1995.
- [9] A. G. Cohen, D. B. Kaplan, and A. E. Nelson, “Effective field theory, black holes, and the cosmological constant,” *Phys. Rev. Lett.*, vol. 82, pp. 4971–4974, Jun 1999.
- [10] D. Pavón, “Holographic dark energy and late cosmic acceleration,” *Journal of Physics A: Mathematical and Theoretical*, vol. 40, no. 25, p. 6865, 2007.
- [11] L. N. Granda and A. Oliveros, “Infrared cut-off proposal for the Holographic density,” *Phys. Lett. B*, vol. 669, pp. 275–277, 2008.
- [12] W. Fischler and L. Susskind, “Holography and cosmology,” *arXiv preprint hep-th/9806039*, 1998.
- [13] M. Li, “A model of holographic dark energy,” *Physics Letters B*, vol. 603, no. 1-2, pp. 1–5, 2004.
- [14] C. Wetterich, “The cosmon model for an asymptotically vanishing time-dependent cosmological “constant”,” *arXiv preprint hep-th/9408025*, 1994.
- [15] O. Bertolami, F. G. Pedro, and M. Le Delliou, “Dark energy–dark matter interaction and putative violation of the equivalence principle from the Abell cluster A586,” *Physics Letters B*, vol. 654, no. 5-6, pp. 165–169, 2007.
- [16] G. Olivares, F. Atrio-Barandela, and D. Pavon, “Observational constraints on interacting quintessence models,” *Physical Review D*, vol. 71, no. 6, p. 063523, 2005.
- [17] E. Di Valentino, A. Melchiorri, O. Mena, and S. Vagnozzi, “Interacting dark energy in the early 2020s: A promising solution to the H0 and cosmic shear tensions,” *Physics of the Dark Universe*, vol. 30, p. 100666, 2020.

- [18] D. Pavon and W. Zimdahl, “Holographic dark energy and cosmic coincidence,” *Physics Letters B*, vol. 628, no. 3-4, pp. 206–210, 2005.
- [19] W. Zimdahl and D. Pavón, “Interacting holographic dark energy,” *Classical and Quantum Gravity*, vol. 24, no. 22, p. 5461, 2007.
- [20] S. Das, P. Majumdar, and R. K. Bhaduri, “General logarithmic corrections to black-hole entropy,” *Classical and Quantum Gravity*, vol. 19, no. 9, p. 2355, 2002.
- [21] S. Das, S. Shankaranarayanan, and S. Sur, “Black hole entropy from entanglement: a review,” *arXiv preprint arXiv:0806.0402*, 2008.
- [22] S. Das, S. Shankaranarayanan, and S. Sur, “Power-law corrections to entanglement entropy of horizons,” *Physical Review D*, vol. 77, no. 6, p. 064013, 2008.
- [23] S. Das, S. Shankaranarayanan, and S. Sur, “Entanglement and corrections to Bekenstein-Hawking entropy,” in *12th Marcel Grossmann Meeting on General Relativity*, pp. 1138–1141, 2 2010.
- [24] N. Radicella and D. Pavón, “The generalized second law in universes with quantum corrected entropy relations,” *Physics Letters B*, vol. 691, no. 3, pp. 121–126, 2010.
- [25] S. Das, S. Shankaranarayanan, and S. Sur, “Entanglement and Corrections to Bekenstein—Hawking Entropy,” in *The Twelfth Marcel Grossmann Meeting: On Recent Developments in Theoretical and Experimental General Relativity, Astrophysics and Relativistic Field Theories (In 3 Volumes)*, pp. 1138–1141, World Scientific, 2012.
- [26] C. Tsallis, “Possible Generalization of Boltzmann-Gibbs Statistics,” *J. Statist. Phys.*, vol. 52, pp. 479–487, 1988.
- [27] M. L. Lyra and C. Tsallis, “Nonextensivity and Multifractality in Low-Dimensional Dissipative Systems,” *Phys. Rev. Lett.*, vol. 80, pp. 53–56, 1998.
- [28] C. Tsallis, R. Mendes, and A. R. Plastino, “The role of constraints within generalized nonextensive statistics,” *Physica A: Statistical Mechanics and its Applications*, vol. 261, no. 3-4, pp. 534–554, 1998.
- [29] G. Wilk and Z. Włodarczyk, “Interpretation of the nonextensivity parameter q in some applications of Tsallis statistics and Lévy distributions,” *Physical Review Letters*, vol. 84, no. 13, p. 2770, 2000.
- [30] C. Tsallis and L. J. L. Cirto, “Black hole thermodynamical entropy,” *Eur. Phys. J. C*, vol. 73, p. 2487, 2013.
- [31] H. Moradpour, “Implications, consequences and interpretations of generalized entropy in the cosmological setups,” *International Journal of Theoretical Physics*, vol. 55, no. 9, pp. 4176–4184, 2016.
- [32] M. Tavayef, A. Sheykhi, K. Bamba, and H. Moradpour, “Tsallis holographic dark energy,” *Physics Letters B*, vol. 781, pp. 195–200, 2018.
- [33] M. A. Zadeh, A. Sheykhi, H. Moradpour, and K. Bamba, “Note on Tsallis holographic dark energy,” *The European Physical Journal C*, vol. 78, no. 11, pp. 1–11, 2018.

- [34] A. A. Aly, “Tsallis Holographic Dark Energy with Granda-Oliveros Scale in (n+1)-Dimensional FRW Universe,” *Advances in Astronomy*, vol. 2019, p. 8138067, 2019.
- [35] V. Srivastava and U. K. Sharma, “Tsallis holographic dark energy with hybrid expansion law,” *Int. J. Geom. Meth. Mod. Phys.*, vol. 17, no. 11, p. 2050144, 2020.
- [36] U. K. Sharma and V. Srivastava, “Tsallis HDE with an IR cutoff as Ricci horizon in a flat FLRW universe,” *New Astron.*, vol. 84, p. 101519, 2021.
- [37] M. A. Zadeh, A. Sheykhi, and H. Moradpour, “Thermal stability of Tsallis holographic dark energy in nonflat universe,” *General Relativity and Gravitation*, vol. 51, pp. 1–20, 2019.
- [38] A. Dixit, U. K. Sharma, and A. Pradhan, “Tsallis holographic dark energy in FRW universe with time varying deceleration parameter,” *New Astronomy*, vol. 73, p. 101281, 2019.
- [39] Y. Aditya, S. Mandal, P. Sahoo, and D. Reddy, “Observational constraint on interacting Tsallis holographic dark energy in logarithmic Brans–Dicke theory,” *The European Physical Journal C*, vol. 79, no. 12, pp. 1–13, 2019.
- [40] A. K. Yadav, “Note on Tsallis holographic dark energy in Brans–Dicke cosmology,” *Eur. Phys. J. C*, vol. 81, no. 1, p. 8, 2021.
- [41] U. K. Sharma, V. C. Dubey, and A. Pradhan, “Diagnosing interacting Tsallis holographic dark energy in the non-flat universe,” *Int. J. Geom. Meth. Mod. Phys.*, vol. 17, no. 02, p. 2050032, 2020.
- [42] A. Saha and S. Ghose, “Interacting Tsallis holographic dark energy in higher dimensional cosmology,” *Astrophys. Space Sci.*, vol. 365, no. 6, p. 98, 2020.
- [43] S. Ghaffari, A. Mamon, H. Moradpour, and A. Ziaie, “Holographic dark energy in Rastall theory,” *Modern Physics Letters A*, vol. 35, no. 33, p. 2050276, 2020.
- [44] A. V. Astashenok and A. S. Tepliakov, “Some models of holographic dark energy on the Randall–Sundrum brane and observational data,” *International Journal of Modern Physics D*, vol. 29, no. 01, p. 1950176, 2020.
- [45] S. Ghaffari, E. Sadri, and A. H. Ziaie, “Tsallis holographic dark energy in fractal universe,” *Mod. Phys. Lett. A*, vol. 35, no. 14, p. 2050107, 2020.
- [46] A. Al Mamon, “Study of Tsallis holographic dark energy model in the framework of fractal cosmology,” *Modern Physics Letters A*, vol. 35, no. 30, p. 2050251, 2020.
- [47] A. Al Mamon, A. H. Ziaie, and K. Bamba, “A generalized interacting Tsallis holographic dark energy model and its thermodynamic implications,” *The European Physical Journal C*, vol. 80, no. 10, pp. 1–12, 2020.
- [48] A. Jawad and A. M. Sultan, “Cosmic Consequences of Kaniadakis and Generalized Tsallis Holographic Dark Energy Models in the Fractal Universe,” *Advances in High Energy Physics*, vol. 2021, 2021.
- [49] S. Nojiri, S. D. Odintsov, and T. Paul, “Different Faces of Generalized Holographic Dark Energy,” *Symmetry*, vol. 13, no. 6, p. 928, 2021.

[50] V. C. Dubey, S. Srivastava, U. K. Sharma, and A. Pradhan, “Tsallis holographic dark energy in Bianchi-I Universe using hybrid expansion law with k-essence,” *Pramana*, vol. 93, no. 5, pp. 1–10, 2019.

[51] V. Chandra Dubey, A. Kumar Mishra, S. Srivastava, and U. Kumar Sharma, “Tsallis holographic dark energy models in axially symmetric space time,” *Int. J. Geom. Meth. Mod. Phys.*, vol. 17, no. 01, p. 2050011, 2020.

[52] M. Abdollahi Zadeh, A. Sheykhi, K. Bamba, and H. Moradpour, “Effects of anisotropy on the sign-changeable interacting Tsallis holographic dark energy,” *Mod. Phys. Lett. A*, vol. 35, no. 09, p. 2050053, 2019.

[53] U. K. Sharma, S. Srivastava, and A. Beesham, “Swampland criteria and cosmological behavior of Tsallis holographic dark energy in Bianchi-III Universe,” *International Journal of Geometric Methods in Modern Physics*, vol. 17, no. 07, p. 2050098, 2020.

[54] M. Korunur, “Tsallis holographic dark energy in Bianchi type-III spacetime with scalar fields,” *Mod. Phys. Lett. A*, vol. 34, no. 37, p. 1950310, 2019.

[55] S. Bhattacharjee, “Interacting tsallis and rényi holographic dark energy with hybrid expansion law,” *Astrophysics and Space Science*, vol. 365, Jun 2020.

[56] Q. Huang, H. Huang, J. Chen, L. Zhang, and F. Tu, “Stability analysis of a Tsallis holographic dark energy model,” *Classical and Quantum Gravity*, vol. 36, no. 17, p. 175001, 2019.

[57] G. Varshney, U. K. Sharma, and A. Pradhan, “Statefinder diagnosis for interacting Tsallis holographic dark energy models with $\omega - \omega'$ pair,” *New Astron.*, vol. 70, pp. 36–42, 2019.

[58] U. K. Sharma and A. Pradhan, “Diagnosing Tsallis holographic dark energy models with statefinder and $\omega - \omega'$ pair,” *Modern Physics Letters A*, vol. 34, no. 13, p. 1950101, 2019.

[59] A. Jawad, S. Rani, and N. Azhar, “Non-flat FRW universe version of Tsallis holographic dark energy in specific modified gravity,” *Modern Physics Letters A*, vol. 34, no. 07n08, p. 1950055, 2019.

[60] N. Zhang, Y.-B. Wu, J.-N. Chi, Z. Yu, and D.-F. Xu, “Diagnosing Tsallis holographic dark energy models with interactions,” *Modern Physics Letters A*, vol. 35, no. 08, p. 2050044, 2020.

[61] U. K. Sharma, V. C. Dubey, and A. Pradhan, “Diagnosing interacting Tsallis holographic dark energy in the non-flat universe,” *International Journal of Geometric Methods in Modern Physics*, vol. 17, no. 02, p. 2050032, 2020.

[62] V. Srivastava and U. K. Sharma, “Statefinder hierarchy for Tsallis holographic dark energy,” *New Astronomy*, vol. 78, p. 101380, 2020.

[63] A. Iqbal and A. Jawad, “Tsallis, Renyi and Sharma–Mittal holographic dark energy models in DGP brane-world,” *Physics of the Dark Universe*, vol. 26, p. 100349, 2019.

[64] A. Mohammadi, T. Golanbari, K. Bamba, and I. P. Lobo, “Tsallis holographic dark energy for inflation,” *Physical Review D*, vol. 103, no. 8, p. 083505, 2021.

- [65] V. C. Dubey and U. K. Sharma, “Comparing the holographic principle inspired dark energy models,” *New Astronomy*, vol. 86, p. 101586, 2021.
- [66] R. D’Agostino, “Holographic dark energy from nonadditive entropy: cosmological perturbations and observational constraints,” *Physical Review D*, vol. 99, no. 10, p. 103524, 2019.
- [67] M. Younas, A. Jawad, S. Qummer, H. Moradpour, and S. Rani, “Cosmological implications of the generalized entropy based holographic dark energy models in dynamical Chern-Simons modified gravity,” *Advances in High Energy Physics*, vol. 2019, 2019.
- [68] W. da Silva and R. Silva, “Cosmological perturbations in the Tsallis holographic dark energy scenarios,” *The European Physical Journal Plus*, vol. 136, no. 5, pp. 1–19, 2021.
- [69] A. A. Aly, “Study of F (T) gravity in the framework of the Tsallis holographic dark energy model,” *The European Physical Journal Plus*, vol. 134, no. 7, pp. 1–7, 2019.
- [70] M. Sharif and S. Saba, “Tsallis Holographic Dark Energy in $f(G,T)$ Gravity,” *Symmetry*, vol. 11, no. 1, 2019.
- [71] A. Jawad, A. Aslam, and S. Rani, “Cosmological implications of Tsallis dark energy in modified Brans–Dicke theory,” *Int. J. Mod. Phys. D*, vol. 28, no. 11, p. 1950146, 2019.
- [72] A. Shaikh, “Diagnosing Renyi and Tsallis Holographic Dark Energy Models with Hubble’s Horizon Cutoff,” *arXiv preprint arXiv:2105.04411*, 2021.
- [73] P. Ens and A. Santos, “ $f (R)$ gravity and Tsallis holographic dark energy,” *EPL (Europhysics Letters)*, vol. 131, no. 4, p. 40007, 2020.
- [74] A. Jawad, S. Hussain, S. Rani, and S. Qummer, “Generalized ghost tsallis holographic dark energy model in rs-ii braneworld and dynamical chern-simons modified gravity,” *International Journal of Geometric Methods in Modern Physics*, vol. 17, no. 08, p. 2050124, 2020.
- [75] A. Jawad and S. Hussain, “Generalized Ghost Tsallis Dark Energy in Modified theories of Gravity,” *International Journal of Geometric Methods in Modern Physics*, 2020.
- [76] M. V. Santhi and Y. Sobhanbabu, “Bianchi type-III Tsallis holographic dark energy model in Saez–Ballester theory of gravitation,” *The European Physical Journal C*, vol. 80, no. 12, pp. 1–15, 2020.
- [77] A. A. Aly, M. A. Elrashied, and M. M. Selim, “Cosmological evolution of Tsallis holographic dark energy model in LTB inhomogeneous gravity,” *International Journal of Modern Physics D*, vol. 29, no. 03, p. 2050023, 2020.
- [78] S. Rani, A. Jawad, K. Bamba, and I. U. Malik, “Cosmological consequences of new dark energy models in Einstein-Aether gravity,” *Symmetry*, vol. 11, no. 4, p. 509, 2019.
- [79] S. H. Shekh, P. H. R. S. Moraes, and P. K. Sahoo, “Physical Acceptability of the Renyi, Tsallis and Sharma-Mittal Holographic Dark Energy Models in the $f(T, B)$ Gravity under Hubble’s Cutoff,” *Universe*, vol. 7, no. 3, p. 67, 2021.

[80] G. Varshney, U. K. Sharma, and A. Pradhan, “Reconstructing the k -essence and the dilation field models of the THDE in $f(R, T)$ gravity,” *Eur. Phys. J. Plus*, vol. 135, no. 7, p. 541, 2020.

[81] U. K. Sharma, “Reconstruction of quintessence field for the THDE with swampland correspondence in $f(R, T)$ gravity,” *arXiv preprint arXiv:2005.03979*, 2020.

[82] G. Varshney, U. K. Sharma, A. Pradhan, and N. Kumar, “Reconstruction of Tachyon, Dirac-Born-Infeld-essence and Phantom model for Tsallis holographic dark energy in $f(R, T)$ gravity,” *Chin. J. Phys.*, vol. 73, p. 1474, 2021.

[83] M. Vijaya Santhi and Y. Sobhanbabu, “Tsallis holographic dark energy models in Bianchi type space time,” *New Astronomy*, vol. 89, p. 101648, 2021.

[84] S. Maity and U. Debnath, “Study of Tsallis, Rényi and Sharma–Mittal holographic dark energies for entropy corrected modified field equations in Hořava–Lifshitz gravity,” *International Journal of Geometric Methods in Modern Physics*, vol. 17, no. 11, p. 2050170, 2020.

[85] Y. Liu, “Tachyon model of Tsallis holographic dark energy,” *Eur. Phys. J. Plus*, vol. 136, no. 5, p. 579, 2021.

[86] M. Zubair and L. R. Durrani, “Exploring tsallis holographic dark energy scenario in $f(R, T)$ gravity,” *Chin. J. Phys.*, vol. 69, pp. 153–171, 2021.

[87] S. Bhattacharjee, “Growth rate and configurational entropy in Tsallis holographic dark energy,” *The European Physical Journal C*, vol. 81, no. 3, pp. 1–8, 2021.

[88] A. Jawad, K. Bamba, M. Younas, S. Qummer, and S. Rani, “Tsallis, Rényi and Sharma–Mittal Holographic Dark Energy Models in Loop Quantum Cosmology,” *Symmetry*, vol. 10, no. 11, 2018.

[89] A. Pradhan and A. Dixit, “Tsallis holographic dark energy model with observational constraints in the higher derivative theory of gravity,” *New Astronomy*, p. 101636, 2021.

[90] A. Lymeris and E. N. Saridakis, “Modified cosmology through nonextensive horizon thermodynamics,” *The European Physical Journal C*, vol. 78, no. 12, pp. 1–11, 2018.

[91] A. Sheykhi, “Modified Friedmann equations from Tsallis entropy,” *Physics Letters B*, vol. 785, pp. 118–126, 2018.

[92] S. Nojiri, S. D. Odintsov, and E. N. Saridakis, “Modified cosmology from extended entropy with varying exponent,” *The European Physical Journal C*, vol. 79, no. 3, pp. 1–10, 2019.

[93] S. Nojiri, S. D. Odintsov, E. N. Saridakis, and R. Myrzakulov, “Correspondence of cosmology from non-extensive thermodynamics with fluids of generalized equation of state,” *Nuclear Physics B*, vol. 950, p. 114850, 2020.

[94] K. Abbasi and S. Gharaati, “A Tsallisian Universe,” *arXiv preprint arXiv:2006.01763*, 2020.

- [95] M. Asghari and A. Sheykhi, “Observational constraints on Tsallis modified gravity,” *arXiv preprint arXiv:2106.15551*, 2021.
- [96] P. George, V. M. Shareef, and T. K. Mathew, “Interacting holographic Ricci dark energy as running vacuum,” *Int. J. Mod. Phys. D*, vol. 28, no. 04, p. 1950060, 2018.
- [97] A. A. Starobinsky, “How to determine an effective potential for a variable cosmological term,” *JETP Lett.*, vol. 68, pp. 757–763, 1998.
- [98] D. M. Scolnic *et al.*, “The Complete Light-curve Sample of Spectroscopically Confirmed SNe Ia from Pan-STARRS1 and Cosmological Constraints from the Combined Pantheon Sample,” *Astrophys. J.*, vol. 859, no. 2, p. 101, 2018.
- [99] H. Yu, B. Ratra, and F.-Y. Wang, “Hubble Parameter and Baryon Acoustic Oscillation Measurement Constraints on the Hubble Constant, the Deviation from the Spatially Flat Λ CDM Model, the Deceleration–Acceleration Transition Redshift, and Spatial Curvature,” *Astrophys. J.*, vol. 856, no. 1, p. 3, 2018.
- [100] H. Amirhashchi and S. Amirhashchi, “Constraining Bianchi Type I Universe With Type Ia Supernova and H(z) Data,” *Phys. Dark Univ.*, vol. 29, p. 100557, 2020.
- [101] D. Pavón and B. Wang, “Le Châtelier–Braun principle in cosmological physics,” *General Relativity and Gravitation*, vol. 41, no. 1, pp. 1–5, 2009.
- [102] G. Hinshaw, J. Weiland, R. Hill, N. Odegard, D. Larson, C. Bennett, J. Dunkley, B. Gold, M. Greason, N. Jarosik, E. Komatsu, M. Nolta, L. Page, D. Spergel, E. J. Wollack, M. Halpern, A. Kogut, M. Limon, S. Meyer, G. Tucker, and E. Wright, “Five-Year Wilkinson Microwave Anisotropy Probe (WMAP) Observations: Data Processing, Sky Maps, & Basic Results,” *Astrophysical Journal Supplement Series*, vol. 180, pp. 225–245, 2008.
- [103] N. Aghanim *et al.*, “Planck 2018 results. VI. Cosmological parameters,” *Astron. Astrophys.*, vol. 641, p. A6, 2020. [Erratum: *Astron. Astrophys.* 652, C4 (2021)].
- [104] E. Sadri, “Observational constraints on interacting Tsallis holographic dark energy model,” *The European Physical Journal C*, vol. 79, no. 9, pp. 1–13, 2019.
- [105] U. Alam, V. Sahni, and A. A. Starobinsky, “The case for dynamical dark energy revisited,” *Journal of Cosmology and Astroparticle Physics*, vol. 2004, no. 06, p. 008, 2004.
- [106] A. Al Mamon and K. Bamba, “Observational constraints on the jerk parameter with the data of the Hubble parameter,” *Eur. Phys. J. C*, vol. 78, no. 10, p. 862, 2018.
- [107] A. A. Mamon, K. Bamba, and S. Das, “Constraints on reconstructed dark energy model from SN Ia and BAO/CMB observations,” *Eur. Phys. J. C*, vol. 77, no. 1, p. 29, 2017.
- [108] A. A. Mamon and S. Das, “A parametric reconstruction of the deceleration parameter,” *Eur. Phys. J. C*, vol. 77, no. 7, p. 495, 2017.
- [109] O. Farooq, F. R. Madiyar, S. Crandall, and B. Ratra, “Hubble Parameter Measurement Constraints on the Redshift of the Deceleration–acceleration Transition, Dynamical Dark Energy, and Space Curvature,” *Astrophys. J.*, vol. 835, no. 1, p. 26, 2017.

- [110] E. Ebrahimi, “A dynamical system analysis of Tsallis holographic dark energy,” *Astrophysics and Space Science*, vol. 365, pp. 1–11, 2020.
- [111] D. Valcin, R. Jimenez, L. Verde, J. L. Bernal, and B. D. Wandelt, “The age of the Universe with globular clusters: reducing systematic uncertainties,” *JCAP*, vol. 08, p. 017, 2021.
- [112] V. Sahni, T. D. Saini, A. A. Starobinsky, and U. Alam, “Statefinder: A New geometrical diagnostic of dark energy,” *JETP Lett.*, vol. 77, pp. 201–206, 2003.
- [113] U. Alam, V. Sahni, T. D. Saini, and A. A. Starobinsky, “Exploring the expanding universe and dark energy using the Statefinder diagnostic,” *Mon. Not. Roy. Astron. Soc.*, vol. 344, p. 1057, 2003.
- [114] R. D. Gregory, *Classical Mechanics*. Cambridge University Press, 2006.
- [115] D. Pavon and N. Radicella, “Does the entropy of the Universe tend to a maximum?,” *Gen. Rel. Grav.*, vol. 45, pp. 63–68, 2013.
- [116] S. M. Crawford, A. L. Ratsimbazafy, C. M. Cress, E. A. Olivier, S.-L. Blyth, and K. J. van der Heyden, “Luminous Red Galaxies in Simulations: Cosmic Chronometers?,” *Mon. Not. Roy. Astron. Soc.*, vol. 406, p. 2569, 2010.
- [117] J. C. Carvalho and J. S. Alcaniz, “Cosmography and cosmic acceleration,” *Mon. Not. Roy. Astron. Soc.*, vol. 418, pp. 1873–1877, 2011.
- [118] J. Simon, L. Verde, and R. Jimenez, “Constraints on the redshift dependence of the dark energy potential,” *Phys. Rev. D*, vol. 71, p. 123001, 2005.
- [119] D. Stern, R. Jimenez, L. Verde, M. Kamionkowski, and S. A. Stanford, “Cosmic Chronometers: Constraining the Equation of State of Dark Energy. I: $H(z)$ Measurements,” *JCAP*, vol. 02, p. 008, 2010.
- [120] B. Wang, Y. Gong, and E. Abdalla, “Thermodynamics of an accelerated expanding universe,” *Phys. Rev. D*, vol. 74, p. 083520, Oct 2006.
- [121] C. A. Egan and C. H. Lineweaver, “A Larger Estimate of the Entropy of the Universe,” *The Astrophysical Journal*, vol. 710, no. 2, p. 1825, 2010.
- [122] K. P. B and T. K. Mathew, “Emergence of cosmic space and the maximization of horizon entropy,” 2 2020.